AGROCIENCIA URUGUAY

Agrociencia Uruguay 2025 | Volume 29 | Article e1636
DOI: 10.31285/AGRO.29.1636
ISSN 2730-5066

Physiological response of *Poncirus trifoliata* rootstock to infection by an RB of Citrus tristeza virus isolate

Rubio, L.[1]; Machado, D.[1]; Otero, A.[1]; Blanco, O.[1]; Guimaraens, A.[1]; Sebres, M.[1]; Colina, R.[2]; Rivas, F.[1]

[1]*Instituto Nacional de Investigación Agropecuaria (INIA), Sistema Vegetal Intensivo, Salto, Uruguay*
[2]*Universidad de la República, Centro Universitario Litoral Norte (CENUR), Laboratorio Virología, Salto, Uruguay*

Editor
Milka Ferrer
Universidad de la República, Montevideo, Uruguay

Received *16 Dec 2024*
Accepted *29 Apr 2025*
Published *12 May 2025*

Correspondence
Leticia Rubio
lrubio@inia.org.uy

Abstract

In citrus growing areas where Citrus tristeza virus (CTV) is endemic, *Poncirus* trifoliata is commonly used as a rootstock to prevent tree decline. However, resistance breaking (RB) CTV isolates, capable of systemically infecting *P. trifoliata*, have been identified. Nevertheless, their effects on the rootstock remain understudied. Therefore, the aim of this work was to evaluate the physiological response of *P. trifoliata* to infection by a local RB isolate (RB-UY1), and determine its effects on grafted scions, using Navel orange (N/*P. trifoliata*) and Mexican lime (ML/*P. trifoliata*) as models. Growth parameters, symptoms expression, photosynthetic activity, and oxidative stress were periodically recorded. The results showed that the photosynthetic activity was not affected by the RB-UY1 isolate in *P. trifoliata* nor in grafted scions. Oxidative damage was not detected in any treatment, despite higher levels of hydrogen peroxide and superoxide radicals in RB-inoculated plants. Nonetheless, a decline in growth was recorded in *P. trifoliata* and ML/*P. trifoliata*, but not in N/*P. trifoliata*. In response to the RB-UY1 infection, there was a significant increase in total phenol concentration in the rootstock and N/*P. trifoliata*; however, enzyme activity of catalase and ascorbate peroxidase did not differ among treatments. In conclusion, infection by the RB-UY1 isolate affected growth rootstock over time, but did not compromise the physiological performance of N/*P. trifoliate* scion. These findings demonstrate a clear host-viral isolate interaction and underscore the need for further studies to elucidate the underlying mechanisms of host response to RB-CTV isolates.

Keywords: citrus, CTV, growth parameters, photosynthesis, resistance breaking isolates

Respuesta fisiológica del portainjerto *Poncirus trifoliata* a la infección por un aislado RB de Citrus tristeza virus

Resumen

En las zonas productoras de cítricos donde el virus de la tristeza de los cítricos (CTV) es endémico, *Poncirus trifoliata* es comúnmente usado como portainjerto para evitar el declinamiento de los árboles. Sin embargo, han sido identificados aislados de CTV que quiebran la resistencia (RB), capaces de infectar sistémicamente a *P. trifoliata*. No obstante, sus efectos sobre el portainjerto han sido poco estudiados. Por lo tanto, el objetivo de este trabajo fue evaluar la respuesta fisiológica de *P. trifoliata* a la infección por un aislado RB local (RB-UY1) y determinar sus efectos sobre la variedad, utilizando naranja navel (N/*P. trifoliata*) y lima mexicana (ML/*P. trifoliata*) como modelos. Periódicamente, se registraron parámetros de crecimiento, expresión de síntomas, actividad fotosintética y estrés oxidativo. Los resultados mostraron

CC BY

Rubio L, Machado D, Otero Á, Blanco O, Guimaraens A, Sebres M, Colina R, Rivas F. Physiological response of Poncirus trifoliata rootstock to infection by an RB of Citrus tristeza virus isolate. Agrociencia Uruguay [Internet]. 2025 [cited dd mmm yyyy];29:e1636. Doi: 10.31285/AGRO.29.1636.

que la actividad fotosintética no fue afectada por el aislado RB-UY1 en *P. trifoliata* ni en las especies injertadas. No se detectó daño oxidativo en ningún tratamiento, a pesar de observar mayores niveles de radicales peróxido de hidrógeno y superóxido en plantas RB-UY1-inoculadas. Sin embargo, se registró una reducción de crecimiento en *P. trifoliata* y ML/*P. trifoliata*, pero no en N/*P. trifoliata*. En respuesta a la infección por RB-UY1, hubo un aumento significativo en el contenido total de fenoles en el portainjerto y N/*P. trifoliata*, aunque no hubo diferencias en la actividad enzimática de catalasa y ascorbato peroxidasa entre tratamientos. En conclusión, la infección por el aislado RB-UY1 afectó, con el tiempo, el crecimiento del portainjerto, pero no comprometió el desempeño fisiológico de la variedad en plantas de N/*P. trifoliata*. Estos hallazgos demuestran una clara interacción huésped-aislado viral y subrayan la necesidad de realizar más estudios para dilucidar los mecanismos subyacentes de la respuesta del huésped a los aislados RB-CTV.

Palabras clave: citrus, CTV, fotosíntesis, parámetros de crecimiento, aislados que quiebran la resistencia

Resposta fisiológica do porta-enxerto *Poncirus trifoliata* a infecção por um isolado RB do Citrus triteza virus

Resumo

Em áreas de cultivo de citros onde o Citrus tristeza virus (CTV) é endêmico, *Poncirus trifoliata* é comumente usado como porta-enxerto para prevenir o declínio das árvores. No entanto, isolados de CTV que quebram a resistência (RB), capazes de infectar sistemicamente *P. trifoliata* foram identificados. Entretanto, seus efeitos sobre o porta-enxerto foram pouco estudados. Portanto, o objetivo deste trabalho foi avaliar a resposta fisiológica de *P. trifoliata* à infecção por um isolado local de RB (RB-UY1) e determinar seus efeitos em mudas enxertadas, usando laranja Navel (N/*P. trifoliata*) e lima mexicana (ML/*P. trifoliata*) como modelos. Parâmetros de crescimento, expressão de sintomas, atividade fotossintética e estresse oxidativo foram registrados periodicamente. Os resultados mostraram que a atividade fotossintética não foi afetada pelo isolado RB-UY1 em *P. trifoliata* nem em mudas enxertadas. Nenhum dano oxidativo foi detectado em nenhum tratamento, apesar de observar níveis mais elevados de peróxido de hidrogênio e radicais superóxido em plantas inoculadas com RB-UY1. No entanto, a redução do crescimento foi registrada em *P. trifoliata* e ML/*P. trifoliata*, mas não em N/*P. trifoliata*. Em resposta à infecção por RB-UY1, houve um aumento significativo no conteúdo fenólico total no porta-enxerto e N/*P. trifoliata*, embora não tenha havido diferenças na atividade enzimática da catalase e da ascorbato peroxidase entre os tratamentos. Em conclusão, a infecção pelo isolado RB-UY1 afetou o crescimento do porta-enxerto ao longo do tempo, mas não comprometeu o desempenho fisiológico do rebento N/*P. trifoliata*. Essas descobertas demonstram uma clara interação entre hospedeiro -isolado viral e ressaltam a necessidade de estudos adicionais para elucidar os mecanismos subjacentes à resposta do hospedeiro aos isolados RB-CTV.

Palavras-chave: citrus, CTV, fotossíntese, parâmetros de crescimento, isolados de quebra de resistência

1. Introduction

Citrus tristeza virus (CTV) is a major pathogen affecting citrus crops, responsible for the death of millions of citrus plants worldwide in the mid-20th century and still limiting citrus production in certain regions[(1)(2)]. CTV belongs to the genus *Closterovirus* (family *Closteroviridae*), and possesses a single-stranded, positive-sense RNA genome[(3)]. It is a phloem-limited pathogen of *Rutaceae* family, mainly of the genus *Citrus*. Infected plants may remain asymptomatic or exhibit a wide range of symptoms, depending on the CTV genotype isolate, rootstock/cultivar combination, and environmental conditions[(1)]. CTV induces three major syndromes: quick decline, stem pitting, and seedling yellows[(2)].

Disease management strategies include the use of certified nurse plant, cross-protection programs, and use of tristeza-tolerant rootstocks[(1)(4)(5)]. In Uruguay, as in other citrus growing areas where CTV is endemic, a high proportion of citrus plants are grafted onto *P. trifoliata* and its hybrids, which confer resistance to CTV decline[(1)]. However, isolates capable of replicating and systemically infecting trifoliate rootstocks have been iden-

tified[6][7][8] and classified as resistance-breaking (RB) strains. Although numerous RB isolates have been reported worldwide[9][10][11][12], limited information is available regarding the physiological response of *P. trifoliata* and grafted scions to RB infection.

Viruses often affect structural and biochemical processes involved in the photosynthetic pathway, disrupting chloroplast function, altering enzyme activity, and affecting carbohydrate metabolism and transport[13][14], giving rise to an increase in reactive oxygen species (ROS) production, cellular damage, and symptoms such as leaf chlorosis, impaired growth or even plant death[15][16][17]. In this infection process, numerous host metabolic responses are triggered and enzymatic and non-enzymatic defense mechanisms can be activated. In *Citrus*, some of these mechanisms have been reported, such as synthesis of antioxidant enzymes (i.e. ascorbate peroxidase, catalase, among others[17][18]), pathogen-related proteins[19] or the activation of the xanthophyll cycle[20].

CTV induces a wide range of physiological and biochemical responses in its hosts[15]. A reduction in photosynthetic activity, and changes in gene expression and protein profile have been reported in Mexican lime (*Citrus aurantifolia*), regardless of the severity of the isolate[21]. Activation of defense mechanisms has been observed, with non-enzymatic (total flavonoids, ascorbic acid, phenolic acid) and enzymatic antioxidants (catalase, superoxide dismutase and peroxidase) showing increased activity[16]. However, despite these responses, oxidative damage has also been observed[21].

The objective of this study was to evaluate the physiological response of *P. trifoliata* to infection with an RB isolate and to determine its effect on grafted scions. To achieve this, two model species were used: navel orange (*Citrus sinensis*) and Mexican lime (*Citrus aurantifolia*). The findings of this study provide valuable insights into the use of *P. trifoliata* in citrus-growing regions where CTV is endemic and RB strains have been reported.

2. Materials and Methods

2.1 Virus isolate, plant material, and experimental conditions

The isolate RB-UY1 was obtained from a CTV field isolate in Uruguay. Its RB phenotype was confirmed by inoculation and multiplication in *P. trifoliata*[11] and its genome was then sequenced by the Sanger method (GenBank accession number OP448604). RB-UY1 was maintained on *P. trifoliata* seedlings in an insect-proof greenhouse according to standard procedures[22].

The physiological response induced by the RB-UY1 isolate was evaluated in three plants model: a) *P. trifoliata* seedlings; b) Mexican lime (ML; *Citrus aurantifolia*) grafted onto *P. trifoliata*; and c) Navel orange (N; *Citrus sinensis*) grafted onto *P. trifoliata*. Five plants of each combination were inoculated with RB-UY1 isolate, while another set (five plants) of uninoculated combinations remained as control.

CTV infection was confirmed by real-time RT-PCR according to the protocol described by Bertolini and others[23]. The experiment was conducted in an insect-proof and temperature-controlled greenhouse (18-24 °C), for 4 years. The plants were kept in 5L pots and the substrate consisted of a mixture of peat and sand. Irrigation and fertilization were carried out according to standard horticultural practices, and the plants were pruned at the same size, once a year, in autumn. Rootstocks were guided to form a single main branch, while the scions were guided to three branches. All plants were placed randomly on the same table, inside the greenhouse.

All measurements were carried out at the same time, every six months, except when some treatments did not have sufficient foliage (example *P. trifoliata*), or for gas exchange parameters, which were measured one time a year.

2.2 Plant growth parameters and CTV symptoms

The length of each branch was measured from the base of the plant to its highest point, and the average height per plant was calculated. For stem diameter determination, measurements were taken at 10 cm above the ground. Leaf area was determined in five randomly selected leaves per plant, and analyzed using a LI-3100 leaf area meter (LICOR, USA). All growth parameters measurements were recorded per plant, and the average for each treatment was subsequently calculated. The presence of CTV visible symptoms such as vein clearing, leaf cupping, vein corking, stunting, and their severity were scored according to Garnsey and others[24]; also, stem pitting was evaluated at the end of experiment.

2.3 Chlorophyll fluorescence parameters

Leaf fluorescence parameters were assessed using an OS5p portable fluorometer (Opti-Sciences, USA) in all plants of each treatment, using three mature leaves per plant randomly selected. Chlorophyll fluorescence parameter *Fv/Fm*, which represents the maximum efficiency of photosystem II (*PSII*) photochemistry, was determined following the procedures of van Kooten and Snell[25], using a modulated light pulse emission after a dark period of 30 min. Quantum yield (*ΦPSII*) was measured in the same leaves after actinic light adaptation. Other variables such as minimum fluorescence (*Fo*), maximum fluorescence (*Fm*), maximum fluorescence under regular PAR (*Fm'*), and non-photochemical quenching (*NPQ*) were analyzed to determine possible changes in different photosynthetic stages. Calculations and terminology were applied as in Kramer and others[26].

2.4 Chlorophyll index

Leaf chlorophyll content was determined using a Chlorophyll Meter SPAD 502 DLPlus (Spectrum Technologies, USA). Measurements were taken on three mature leaves, from all plants in each treatment.

2.5 Gas exchange parameters

Leaf gas exchange parameters were measured with a CIRAS-3 portable gas analyzer (PP Systems, USA) under ambient CO_2 and humidity. Supplemental light was provided by a PAR lamp with a photon flux density of 1200 µmol m^{-2} s^{-1}, and air flow was set at 300 µmol s^{-1}. Measurements were taken on three mature leaves from all plants in each treatment. Net CO_2 assimilation rate (*A*; µmol $m^{-2}s^{-1}$), ratio of intracellular to ambient CO_2 concentration (*Ci/Ca*), stomatal conductance (*gs*; mol m^{-2} s^{-1}), and transpiration rate (*E*) were evaluated. Leaf-to-air vapor pressure difference was calculated from cuvette air temperature, relative humidity, and cuvette *TL*, assuming that leaf water was saturated at *TL*. Ci/Ca was calculated from leaf internal CO_2 partial pressure (Ci).

2.6 Determination of malondialdehyde, hydrogen peroxide, and superoxide radicals in plant tissues

The concentration of malondialdehyde (MDA) was determined following the method described by Dhindsa and Matowe[27]. In this procedure, leaf tissue (250mg) was ground using liquid nitrogen and homogenized in 0.1% trichloroacetic acid (TCA; Merck KGaA), filtered, and maintained on ice. The reaction was initiated by adding an equal volume of 0.1% thiobarbituric acid (TBA; Merck KGaA) prepared in 20% TCA. The mixture was then incubated at 95 °C for 30 minutes, followed by rapid cooling on ice and centrifugation. The supernatant was analyzed by spectrophotometry at 440, 534, and 600 nm, and the MDA concentration was calculated according to the formula proposed by the original authors.

To evaluate oxidative stress, the accumulation of hydrogen peroxide (H_2O_2) and superoxide radicals (O_2-) was assessed through histological staining, based on the methodology of Ramel and others[28], with slight modifications. The presence of O_2- was detected using thiazolyl blue tetrazolium bromide (MTT; Sigma, St.

Louis), whereas H_2O_2 accumulation was visualized using 3,3'-diaminobenzidine (DAB; Sigma, St. Louis) staining. In both cases, leaf discs were incubated in the respective staining solutions for four hours in the dark. After incubation, the samples were subjected to a bleaching process in a mixture of acetic acid, glycerol, and ethanol (1/1/3) (v/v/v) at 100 °C, followed by preservation in a glycerol-ethanol solution. The stained tissues were subsequently photographed to document the distribution of reactive oxygen species. To quantify these compounds, the leaves were pulverized in liquid nitrogen, and the extracted pigments were solubilized in either DMSO for O_2- detection or $HClO_4$ for hydrogen peroxide analysis. The absorbance of the solutions was then measured at 570 nm for O_2- and 405 nm for H_2O_2, using appropriate blanks for reference.

2.7 Determination of total phenolic content and enzyme activity

Total phenolic content and enzyme activity were analyzed to assess the plant response to RB-UY1-CTV infection at the end of the experiment. Phenolic compounds were quantified using the Folin-Ciocalteu reagent method[29]. In brief, lyophilized leaf samples (50 mg) were extracted with methanol at 80%, homogenized, and centrifuged. The resulting supernatant was then mixed with the Folin-Ciocalteu reagent and incubated for 3 min. Finally, sodium carbonate was added, and after incubation in darkness for 2 hours, absorbance was measured at 760 nm. A gallic acid standard curve was constructed, and the total phenols content in the samples was calculated by extrapolation absorbance values to the calibration curve.

To evaluate antioxidant enzyme activity, ascorbate peroxidase (APX) and catalase (CAT) activities were measured using spectrophotometric assays. Enzyme extracts were obtained by homogenizing ground tissue (250 mg) in potassium phosphate buffer (100 mM, PH=7.0), followed by centrifugation. Protein concentration in the extracts was determined using the Bradford method[30], with bovine serum albumin (Sigma-Aldrich) as the standard. CAT activity was determined by quantifying the decrease in absorbance at 240 nm (E = 39.4 mM^{-1} cm^{-1}). The reaction mixture included the plant extract, potassium phosphate buffer (100mM), and H_2O_2 (100mM, Sigma-Aldrich). The reaction was initiated by adding H_2O_2[31] and the absorbance was recorded at 1-minute intervals over 4 minutes. APX activity was evaluated by monitoring the decrease in absorbance at 290 nm (E = 2.8 mM^{-1} cm^{-1}) in a reaction mixture containing plant extract, potassium phosphate buffer (100mM), ascorbic acid (0.5mM, Sigma-Aldrich), and H_2O_2 (4mM, Sigma-Aldrich). Absorbance values were recorded at 2 and 5 minutes[32].

2.8 Statistical analysis

Data were processed using R software, version 4.2.3. Data normality was analyzed by Shapiro-Wilk test. According to this, data were processed by mixed linear model. The means of the different variables were compared between treatments (control vs. inoculated plants, in each model plants); least significant difference was determined by Tukey test at $p \leq 0.05$.

3. Results

3.1 Plant growth and CTV symptoms

The presence of the virus was confirmed in inoculated plants approximately one year after inoculation by real-time RT-PCR. Consequently, this time point was considered as the baseline for infection in the data analysis. Regarding growth variables, plant height and leaf area were significantly reduced in RB-inoculated *P. trifoliata* and ML/*P. trifoliata* plants compared to control plants, 48 months post-inoculation. In contrast, growth in RB-inoculated N/*P. trifoliata* plants remained unaffected by virus infection, although a slight initial growth restriction was observed, but the difference was not statistically significant compared to the control plants (**Figure 1**).

Foliar symptoms associated with CTV were observed exclusively in ML/*P. trifoliata* plants, which exhibited mild vein clearing and leaf cupping, both classified as mild symptoms of the disease. However, by the end of the experimental period, RB-inoculated *P. trifoliata* plants showed mild to moderate stem pitting (**Figure 2.**).

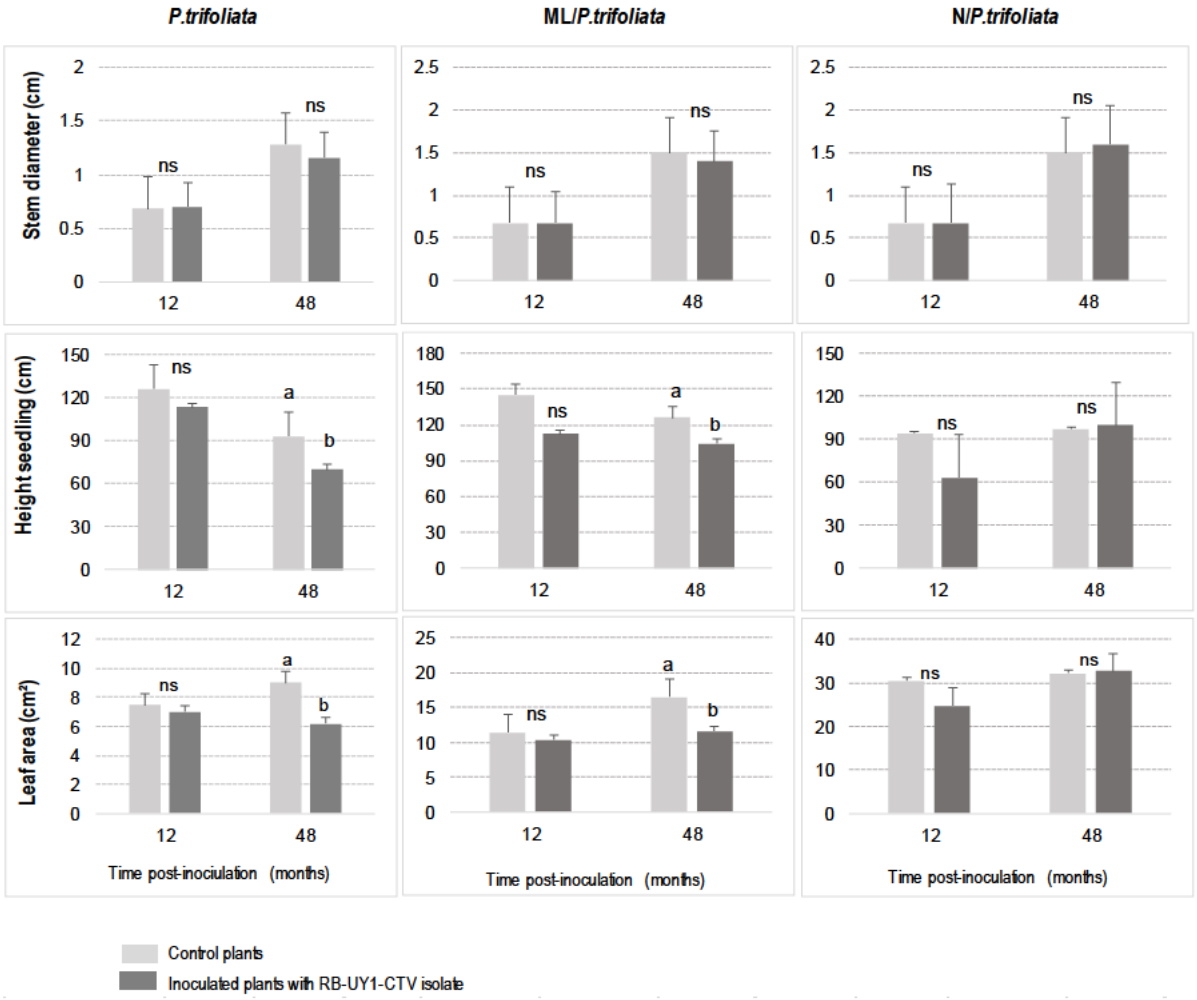


Figure 1. Growth parameters evaluated in *P. trifoliata* seedlings, ML/*P. trifoliata*, and N/*P. trifoliata* at 12 and 48 months post-inoculation with RB-UY1-CTV isolate

Parameters: Stem diameter (cm), Height seedling (cm), and Leaf area (cm²/leaf). Data are mean values of five independent measures and twenty-five leaves in each treatment ± standard error. Different letters denote significant differences at $P \leq 0.05$; ns: not significant differences.



Figure 2. Symptoms produced by RB-UY1-CTV isolate

A: mild vein clearing in ML/*P. trifoliata*; B: leaf cupping in ML/*P. trifoliata*; C: Left: healthy bark in *P. trifoliata* control; Right: stem pitting induced by RB-UY1-CTV isolate in *P. trifoliata*

3.2 Chlorophyll fluorescence parameters

The maximum fluorescence yield in dark-adapted leaves (*Fv/Fm*) remained stable at approximately 0.8 in all treatments throughout the experiment, regardless of plant species or virus infection (**Figure 3**; 1A, 1B, 1C). Similarly, the quantum yield efficiency in light-adapted leaves (*ΦPSII*) was not affected (**Figure 3**; 2A, 2C, 2B). Despite of this, a slight decreasing trend was observed for this parameter in RB-inoculated ML/*P. trifoliata* plants by the third year post-inoculation.

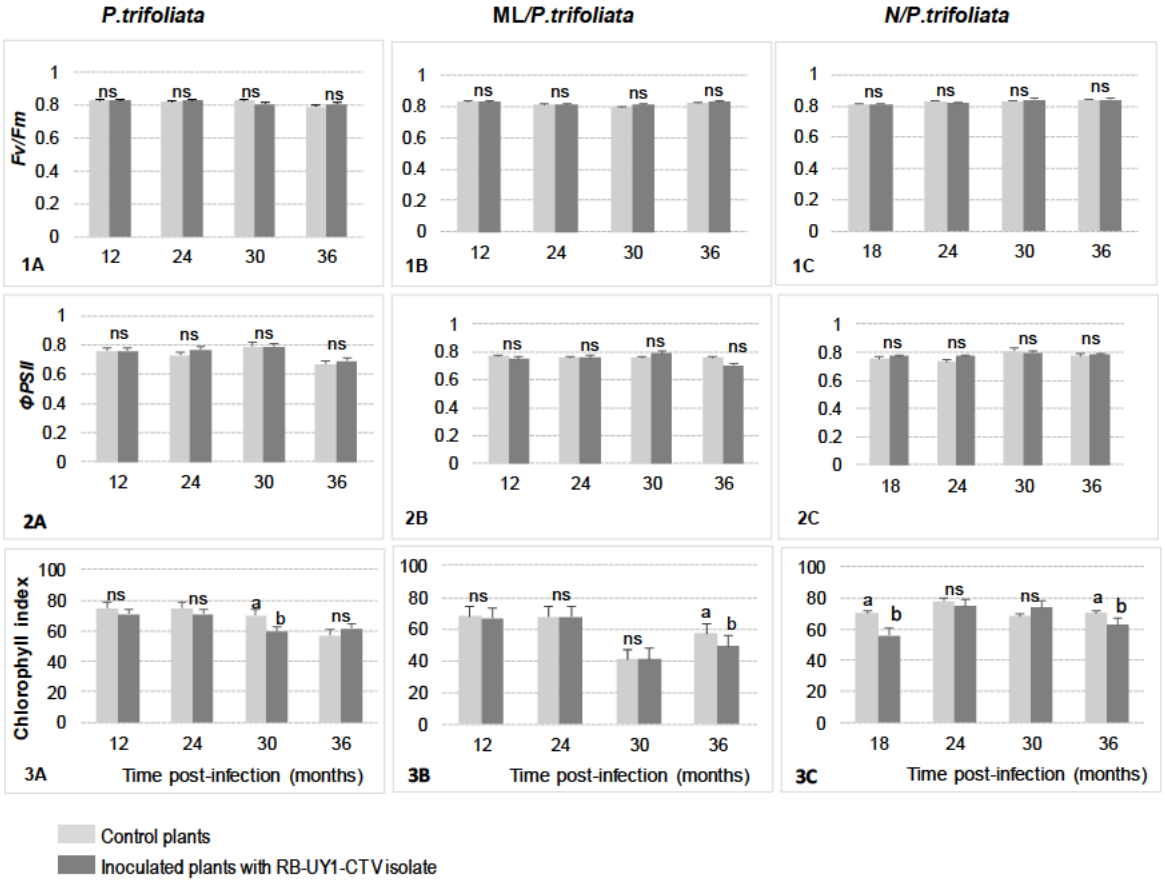


Figure 3. Evaluation of chlorophyll fluorescence parameters and chlorophyll index in *P. trifoliata* seedlings (A), ML/*P. trifoliata* (B), and N/*P. trifoliata* (C) post-infection with RB-UY1-CTV isolate

Parameters: 1- Maximum fluorescence yield in dark-adapted leaves (*Fv/Fm*); 2- Quantum yield in light-adapted leaves (*ΦPSII*). 3- Chlorophyll index. Data are the mean values of 15 independent measurements ± standard error. Different letters denote significant differences at *P≤0.05*; ns: not significant differences

3.3 Leaf chlorophyll index

This parameter showed a slight tendency to decrease in RB-inoculated plants, and was significantly lower in ML/*P. trifoliata* and N/*P. trifoliata* plants at the last assessment (**Figure 3**; 3B, 3C).

3.4 Gas exchange parameters

The leaf net assimilation rate (*A*) did not show significant differences between RB-inoculated and non-inoculated plants throughout the experimental period. However, a reduction in *A* was observed in ML/*P. trifoliata* in the last evaluation (**Figure 4**; 1A, 1B, 1C). The stomatal conductance (*gs*) and *Ci/Ca* ratio were generally higher in RB-inoculated plants during the early stages of infection (up to 24 months), with *P. trifoliata* exhibiting the most marked response (**Figure 4**; 2A, B; 3A, B). Conversely, in RB-inoculated N/*P. trifoliata* plants, *gs* and *Ci/Ca* ratio were lower during the first year post-inoculation (**Figure 4**; 2C, 3C), but exhibited a similar

trend to *P. trifoliata* and ML/*P. trifoliata* at 24 months. By the end of the experiment, gas exchange variables showed no significant differences associated with the presence of the virus.

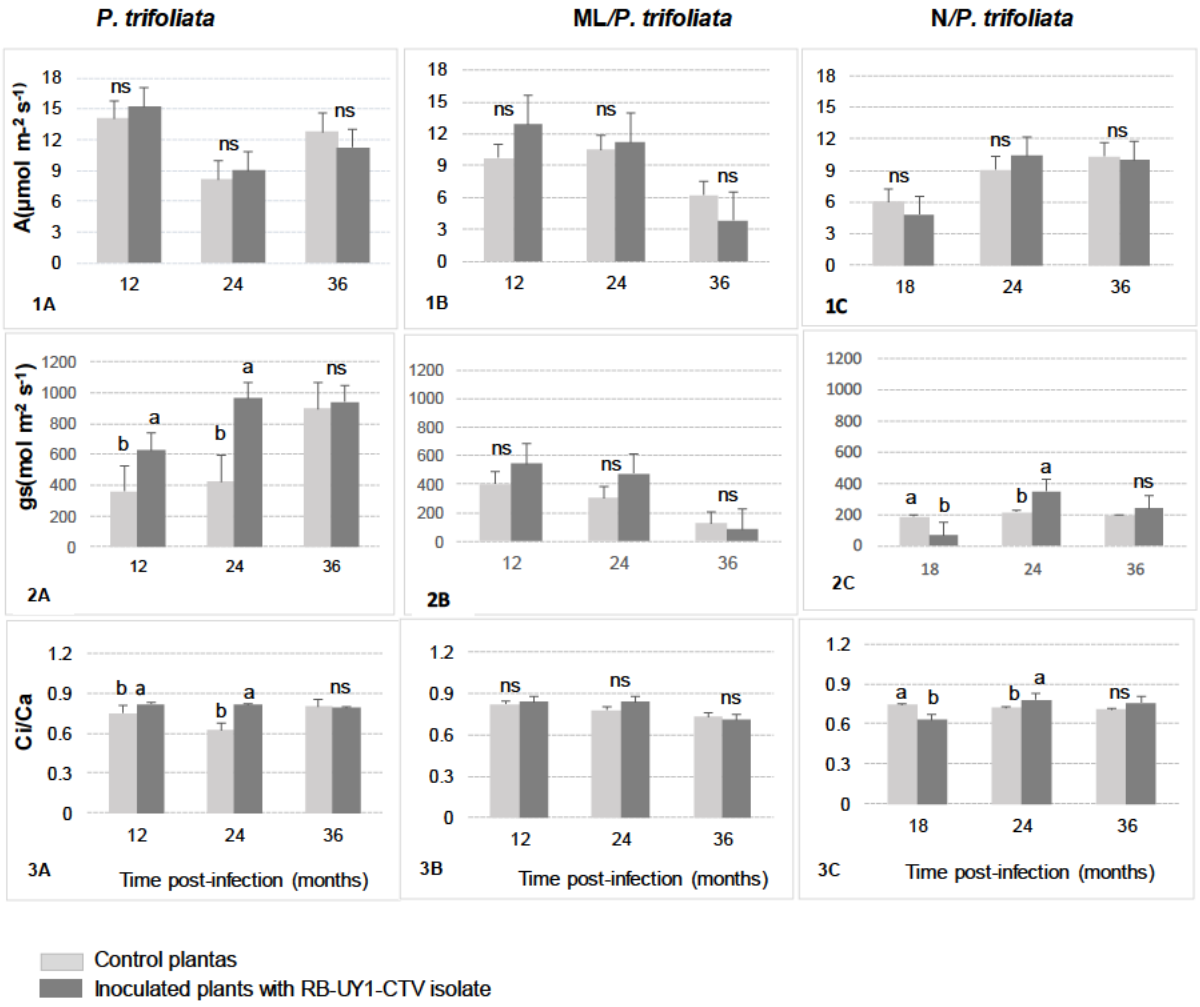


Figure 4. Evaluation of gas exchange parameters in *P. trifoliata* seedlings (A), ML/*P. trifoliata* (B), and N/*P. trifoliata* (C) post-infection with RB-UY1-CTV isolate

Parameters: 1- Leaf net CO_2 assimilation rate (*A*); 2- Stomatal conductance (*gs*); 3- Relation between intracellular and environmental CO_2 concentration (*Ci/Ca*). Data are mean values of 15 independent measurements ± standard error. Different letters denote significant differences at $P \leq 0.05$; ns: not significant differences.

3.5 Oxidative damage and ROS in plant tissues

Oxidative damage in response to infection with the RB-UY1 isolate was assessed by measuring MDA concentration in leaf tissue. No significant differences were observed in this parameter between inoculated and control plants in any of the evaluated species (**Figure 5**). Regarding H_2O_2 and O_2^- concentrations at the end of the experimental period, staining leaf tissues of RB-inoculated plants showed significantly higher absorbance values at 570 nm compared to control plants, indicating a higher concentration of the O_2^- radical. Additionally, RB-inoculated N/*P. trifoliata* plants exhibited higher absorbance at 405 nm than control plants, indicating a significantly higher H_2O_2 content (**Figure 6**). However, these plants also showed staining in the cut area of the leaf tissue (picture in **Figure 6**); likely, the oxidative stress generated there may have also contributed to the increased radical levels.

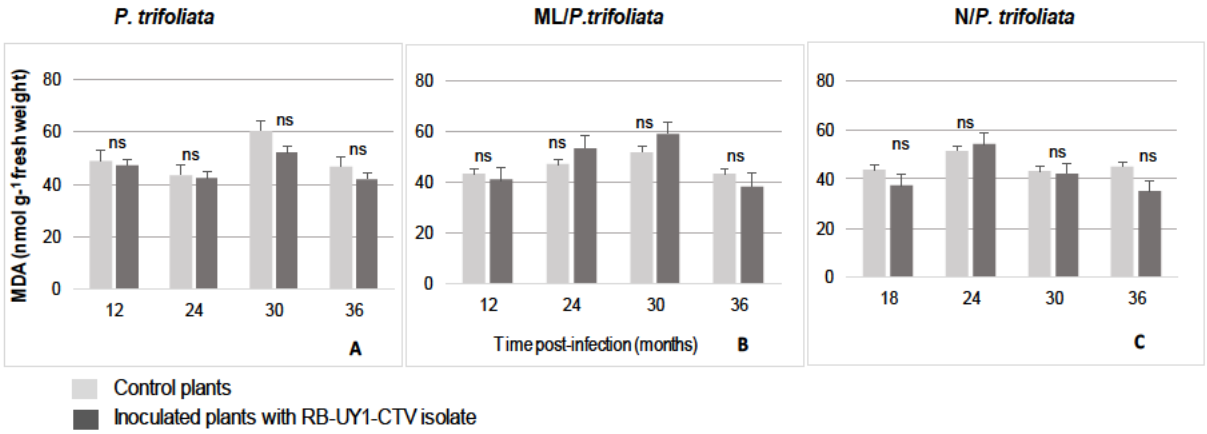


Figure 5. Oxidative damage in response to infection by the RB-UY1-CTV isolate assessed by Malondialdehyde (MDA) concentration in leaf tissue of *P. trifoliata* seedlings (A), ML/*P. trifoliata* (B), and N/*P. trifoliata* (C)

Data are mean values of five replicates ± standard error. Different letters denote significant differences at $P \leq 0.05$, ns: not significant differences

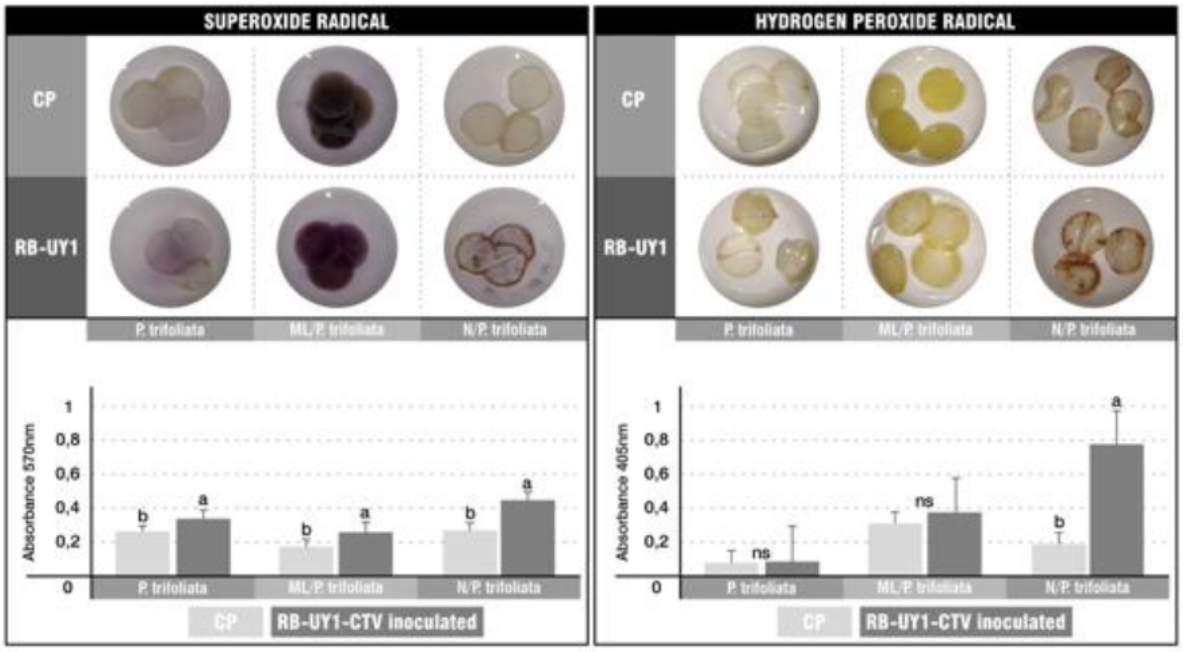


Figure 6. Evaluation of oxidative stress quantifying superoxide and hydrogen peroxide radicals by histological staining method in discs leaf of *P. trifoliata*, ML/*P. trifoliata* and N/*P. trifoliata*, in control (CP) and inoculated (RB-UY1) plants, 36 months post-infection with RB-UY1-CTV isolate

On the top, picture with discs leaf staining with MTT (left) for superoxide determination and with DAB (right) for hydrogen peroxide determination, in each treatment. Absorbance data, at 570nm and 405nm, respectively, are the means of three replicates ± standard error. Different letters denote significant differences at $P \leq 0.05$; ns: not significant differences.

3.6 Total phenolic content and ROS scavenging enzymes

The total phenolic content was significantly higher in RB-inoculated *P. trifoliata* and N/*P. trifoliata* plants (**Table 1**). In contrast, no statistically significant differences were found in enzymatic activity for APX and CAT among control and RB-inoculated plants (**Table 1**).

Table 1. Plant antioxidant response to infection by the RB-UY1-CTV isolate evaluated through the total phenolic content and ascorbate peroxidase (APX) and catalase (CAT) activities in leaf tissue of *P. trifoliata*, ML/*P. trifoliata*, and N/*P. trifoliata*, control and inoculated (RB-UY1) plants at the end of the experiment (36 months post-infection)

	Total phenol content	**Enzyme activity** (µmol mL^{-1} min^{-1})	
Treatment	mg Gallic acid/100g leaf tissue	**APX**	**CAT**
P. trifoliata	559 b ± 17	0.07 a ± 0.008	13.8 a ± 1.5
P. trifoliata + RB-UY1	962 a ± 22	0.11 a ± 0.02	23.4 a ± 2.7
ML/*P. trifoliata*	1273 a ± 4	0.11 a ± 0.008	16.8 a ± 2.2
ML/*P. trifoliata* +RB-UY1	1331 a ± 7	0.08 a ± 0.01	19.3 a ± 1.7
N/*P. trifoliata*	1525 b ± 17	0.03 a ± 0.003	21.2 a ± 1.2
N/*P. trifoliata* + RB-UY1	2117 a ± 25	0.05 a ± 0.006	11.8 a ± 1.3

Data are the means values of three replicates ± standard error. Different letters denote significant differences at $P \leq 0.05$.

4. Discussion

P. trifoliata was the only genotype resistant to most CTV strains until the RB strain was identified. Consequently, this rootstock is widely used in citrus growing regions where the virus is endemic. The RB-UY1 isolate was the first RB isolate reported in Uruguay[11] and it was biologically characterized on indicator plants as a mild isolate[33]. However, CTV isolates are known to exhibit different biological responses depending on the host species, scion-rootstock combinations, infection timing, and environmental conditions[1][15]. Therefore, the RB-UY1 isolate could affect the performance of *P. trifoliata*.

As expected, bioassays revealed that RB-inoculated *P. trifoliata* and N/*P. trifoliata* plants did not exhibit foliar symptoms associated with CTV infection. The virus generally does not induce foliar symptoms in N/*P. trifoliata* plants, and most RB isolates characterized worldwide cause asymptomatic infections in *P. trifoliata*[7][9]. Instead, mild symptoms were observed in ML, the most susceptible species to CTV, confirming RB-UY1 as a mild isolate. However, mild to moderate stem pitting was observed in *P. trifoliata* four years post-inoculation; this symptom is commonly associated with reduced growth and yield of affected plants[15]. The stem pitting observed exclusively in the rootstock can be attributed to the specific interaction between RB strains and trifoliate rootstocks[15][34], as its manifestation and severity depends on the differential expression of p33, p18, and p13 CTV genes in the host species[35][36]. Nevertheless, reports from China and Southern Africa indicate that RB strains have also induced stem pitting in sweet orange, grapefruit, and lime plants[12][37].

Despite the absence of visible symptoms, all viral infections represent a stress for the plant and affect its normal metabolism. Some studies have indicated that the photosynthetic capacity of ML plants may be reduced by CTV infection[21]. However, other studies have demonstrated that long-term infections do not induce significant changes in this process[38]. Our results indicate that the photosynthetic activity of *P. trifoliata* and the grafted species was not affected by infection with the RB-UY1 isolate. The photochemical efficiency, expressed as *Fv/Fm*, remained at approximately 0.8 across all treatments, indicating that the plants were able to grow under optimal physiological conditions[39]. Conversely, previous studies have reported a decrease in *Fv/Fm* and *ΦPSII* in ML infected with CTV, attributing this effect to alterations in the electron transport and a possible photoinhibition process[21]. The RB-UY1 isolate only affected the chlorophyll index, inducing a significant reduction in ML/*P. trifoliata* and N/*P. trifoliata* plants four years post-inoculation. This could have reduced the efficiency of the light-harvesting complexes[21]. However, the absence of changes in *Fo* values suggest that the antenna complex was not damaged and that energy capture was not compromised. Therefore, the RB-UY1 isolate had no significant impact on chlorophyll fluorescence parameters.

Furthermore, viral infection can also affect the mechanism involved in CO_2 assimilation, such as stomatal opening and mesophyll diffusion[40]. In our experiment, RB-inoculated plants exhibited higher stomatal conductance and CO_2 availability within the sub-stomatal cells (*Ci*), during the early stages of infection. Therefore, there would be no discernible limitations in CO_2 assimilation between inoculated and control plants. According to Pérez-Clemente and others[41] the increased stomatal conductance observed in CTV-infected plants is a consequence of the lower abscisic acid (ABA) levels, in order to prioritize defense signaling pathways increasing the production of salicylic and jasmonic acid. However, when *A* was negatively affected by the RB-UY1 isolate in N/*P. trifoliata* plants at the beginning of the experiment and in ML/*P. trifoliata* plants at the end of it, a reduction in *gs* was observed. This indicates that limitations in CO_2 availability and/or diffusion contributed to a decreased rate of CO_2 fixation. In these instances, lower *Ci/Ca* values were recorded, evidencing the presence of stomatal limitations. Pérez-Clemente and others[21], on the other hand, observed a reduction in *A* and *gs* values in CTV-inoculated ML; however, this was accompanied by an increase in the *Ci/Ca* ratio, which was attributed to a decline in carboxylative efficiency. Conversely, Hančević and others[38] did not detect alterations in leaf gas exchange parameters or chlorophyll content in CTV-inoculated ML over an extended period (10 years). These authors assume that in long-term infections regulatory mechanisms may exist between the host and the virus, allowing both to coexist, which is consistent with our results since some parameters were altered only in early stages of infection. Recent studies suggest a potential trade-off between photosynthetic activity and defense against pathogens, mediated by stomatal anatomy[42] and the hormonal regulation.

Regarding oxidative damage, as indicated by MDA levels, no evidence of oxidative burst was observed in any of the treatments. Although higher levels of H_2O_2 and O_2^- radicals were detected in RB-inoculated plants, these did not result in cellular damage. However, these values may have been overestimated due to oxidative stress induced by leaf discs cutting during staining procedure. It is also likely that antioxidant mechanisms were activated, contributing to the prevention of oxidative damage. Indeed, RB-inoculated N/*P. trifoliata* and the rootstock exhibited a significantly increased concentration of phenolic compounds, consistent with the findings of Munir and others[43], who reported that elevated phenolic content may serve as an antioxidant response to CTV in sweet oranges. These compounds can restrict viral movement, generate defense signals, and neutralize oxidative stress, among other functions[44]. In contrast, no increase in phenolic content was observed in RB- inoculated ML/*P. trifoliata* plants. This response is characteristic of susceptible hosts, which often exhibit lower production of secondary metabolites[45]. With respect to antioxidant enzyme activity, no significant differences in APX or CAT levels were observed across treatments. However, the involvement of other antioxidant enzymes cannot be excluded. Previous studies have reported changes in superoxide dismutase (SOD) and polyphenol oxidase (PPO) activity in response to CTV infection[16][38].

The growth parameters, specifically plant height and leaf area, were significantly affected in RB-inoculated *Poncirus trifoliata* and ML/*P. trifoliata* plants four years post-inoculation. However, no such effects were observed in N/*P. trifoliata* plants. Since photosynthetic parameters remained unchanged and there was no evidence of oxidative damage, we inferred that growth limitations were not due to reduced carbohydrate synthesis. Instead, these constraints are more likely attributable to disruptions in carbohydrate transport, alterations in their metabolism, or even hormonal imbalances[46][47]. A critical factor contributing to this limitation could be stem pitting formation, as it induces changes in cell differentiation and development[35], leading to abnormal phloem formation, which interfere with the normal transport of carbohydrates. Moreover, recent studies have confirmed that during stem pitting formation, CTV also invades xylem cells[5]. Consequently, stem pitting can disrupt the transport of carbohydrates, nutrients, and water, affecting plant growth. These findings reinforce the hypothesis that growth limitations in plants infected with RB-UY1 are primarily associated with disruptions in resource transport due to structural modifications in the phloem and xylem, rather than a deficiency in carbohydrate production. In contrast, N/*P. trifoliata* plants exhibited no symptoms or physiological alterations in the scion, consistent with field trials on grapefruit trees, where RB isolates did not negatively impact plant perfor-

mance despite achieving high viral loads[37]. Therefore, the results suggest a clear interaction between genotype-host and viral isolate (RB-UY1), likely mediated by differential gene expression in either the host or virus, or by variations in the virus's ability to move and colonize host tissues[15][36]. Further studies of the host response to infection are required to elucidate the metabolic and genetic pathways involved in the interaction between *P. trifoliata* and RB-CTV.

5. Conclusions

This study demonstrated that the photosynthetic activity was not affected by the RB-UY1 isolate in *P. trifoliata* nor grafted species. Additionally, no evidence of oxidative damage attributable to viral infection was detected, despite increased levels of H_2O_2 and O_2- radicals in RB-UY1 inoculated plants. Nonetheless, a significant reduction in growth was observed in *P. trifoliata* and LM/*P. trifoliata*, while no such decline occurred in N/*P. trifoliata*. Notably, these rootstock growth limitations did not compromise the physiological performance of the N/*P. trifoliata* scion, providing strong evidence of a clear host-viral isolate interaction. Our results suggest that growth reductions are primarily associated with alterations in carbohydrate transport and metabolism, likely due to the presence of stem pitting. In response to the RB-UY1 infection, a significant increase in phenol concentration was detected in the rootstock and N/*P. trifoliate* plants. However, no significant changes were observed in the enzyme activity of catalase and ascorbate peroxidase. This study represents the first comprehensive assessment of the effects of RB-CTV infection in *P. trifoliata* and a commercially relevant sweet orange scion, providing evidence of long-term physiological alterations in the rootstock. Further research is necessary to elucidate the molecular and physiological mechanisms underlying the host response to RB-CTV infection.

Acknowledgements

We thank the citrus sanitation, diffusion and plant protection INIA teams for providing facilities and support for this work. We also thank Mercedes García Roche for reviewing the writing of this manuscript. This research was funded by the National Institute of Agricultural Research (INIA), Uruguay (project CT-22), through the National Program of Citrus Research.

Transparency of data

The dataset supporting the findings of this study is available from the corresponding author upon request.

Author contribution statement

	L Rubio	D Machado	Á Otero	O Blanco	A Guimaraens	M Sebres	R Colina	F Rivas
Conceptualization	■		■				■	■
Data curation	■	■	■	■	■	■		
Formal analysis	■					■		
Investigation	■		■				■	■
Methodology	■	■	■	■	■	■	■	■
Writing – original draft	■							■
Writing – review and editing	■							■

References

(1) Moreno P, Ambrós S, Albiach-Martí MR, Guerri J, Peña L. Citrus tristeza virus: a pathogen that changed the course of the citrus industry. Mol Plant Pathol. 2008;9(2):251-68. Doi: 10.1111/j.1364-3703.2007.00455.x.

(2) Dawson WO, Bar-Joseph M, Garnsey SM, Moreno P. Citrus tristeza virus: making an ally from an enemy. Annu Rev Phytopathol. 2015;53:137-55. Doi: 10.1146/annurev-phyto-080614-120012.

(3) Karasev AV, Boyko VP, Gowda S, Nikolaeva OV, Hilf ME, Koonin EV, Niblett CL, Cline K, Gumpf DJ, Lee RF, Garnsey SM, Lewandowski DJ, Dawson WO. Complete sequence of the citrus tristeza virus RNA genome. Virology. 1995;208(2):511-20. Doi: 10.1006/viro.1995.1182.

(4) Folimonova SY, Achor D, Bar-Joseph M. Walking together: cross-protection, genome conservation, and the replication machinery of Citrus tristeza virus. Viruses. 2020;12(12):1353. Doi: 10.3390/v12121353.

(5) Folimonova SY, Sun YD. Citrus Tristeza virus: from pathogen to panacea. Annu Rev Virol. 2022;9(1):417-35. Doi: 10.1146/annurev-virology-100520-114412.

(6) Albiach-Marti M, Grosser J, Gowda S, Mawassi M, Satyanarayana T, Garnsey S, Dawson W. Citrus tristeza virus replicates and forms infectious virions in protoplasts of resistant citrus relatives. Mol Breed. 2004;14:117-28. Doi: 10.1023/B:MOLB.0000038000.51218.a7.

(7) Harper SJ, Dawson TE, Pearson MN. Isolates of Citrus tristeza virus that overcome Poncirus trifoliata resistance comprise a novel strain. Arch Virol. 2010;155(4):471-80. Doi: 10.1007/s00705-010-0604-5.

(8) Yokomi RK, Selvaraj V, Maheshwari Y, Saponari M, Giampetruzzi A, Chiumenti M, Hajeri S. Identification and characterization of Citrus tristeza virus isolates breaking resistance in Trifoliate Orange in California. Phytopathology. 2017;107(7):901-8. Doi: 10.1094/PHYTO-01-17-0007-R.

(9) Roy A, Choudhary N, Hartung JS, Brlansky RH. The prevalence of the Citrus tristeza virus Trifoliate Resistance breaking genotype among Puerto Rican isolates. Plant Dis. 2013;97(9):1227-34. Doi: 10.1094/PDIS-01-12-0012-RE.

(10) Scott KA, Hlela Q, Zablocki O, Read D, van Vuuren S, Pietersen G. Genotype composition of populations of grapefruit-cross-protecting citrus tristeza virus strain GFMS12 in different host plants and aphid-transmitted sub-isolates. Arch Virol. 2013;158(1):27-37. Doi: 10.1007/s00705-012-1450-4.

(11) Hernández-Rodríguez L, Bertalmío A, Arruabarrena A, Rubio L, Rivas F, Benítez-Galeano MJ, Colina R, Maeso D. First report of the Citrus tristeza virus trifoliate resistance-breaking (RB) genotype in 'Newhall' sweet Orange in South America. Plant Dis. 2017;101(6):1063. Doi: 10.1094/PDIS-04-16-0430-PDN.

(12) Wang J, Zhou T, Cao M, Zhou Y, Li Z. First report of Citrus tristeza virus trifoliate resistance-breaking (RB) genotype in Citrus grandis in China. J Plant Pathol. 2019;101(2):451. Doi: 10.1007/s42161-018-0169-9.

(13) Hull R. Virus-plant interactions in non-permissive and permissive host. In: Plant Virology. 5th ed. London: Academic Press; 2014. p. 605-68.

(14) Jiang T, Zhou T. Unraveling the mechanisms of virus-induced symptom development in plants. Plants (Basel). 2023;12(15):2830. Doi: 10.3390/plants12152830.

(15) Dawson WO, Garnsey SM, Tatineni S, Folimonova SY, Harper SJ, Gowda S. Citrus tristeza virus-host interactions. Front Microbiol. 2013;4:88. Doi: 10.3389/fmicb.2013.00088.

(16) Dória MS, Sousa AO, Barbosa Cde J, Costa MG, Gesteira Ada S, Souza RM, Freitas AC, Pirovani CP. Citrus tristeza virus (CTV) causing proteomic and enzymatic changes in sweet orange variety "Westin". PLoS One. 2015;10(7):e0130950. Doi: 10.1371/journal.pone.0130950.

(17) Arbona V, Flors V, Jacas J, García-Agustín P, Gómez-Cadenas A. Enzymatic and non-enzymatic antioxidant responses of Carrizo citrange, a salt-sensitive citrus rootstock, to different levels of salinity. Plant Cell Physiol. 2003;44(4):388-94. Doi: 10.1093/pcp/pcg059.

(18) Rivas F, Fornes F, Rodrigo M, Zacarías L, Agustí M. Girdling induces oxidative damage and triggers enzymatic and non-enzymatic antioxidative defences in Citrus leaves. Environ Exp Bot. 2008;64(3):256-63. Doi: 10.1016/j.envexpbot.2008.07.006.

(19) van Loon LC, Rep M, Pieterse CM. Significance of inducible defense-related proteins in infected plants. Annu Rev Phytopathol. 2006;44:135-62. Doi: 10.1146/annurev.phyto.44.070505.

(20) Rivas F, Fornes F, Rodrigo M, Zacarías L, Agustí M. Changes in carotenoids and ABA content in Citrus leaves in response to girdling. Sci Hortic. 2011;127:482-7. Doi: 10.1016/j.scienta.2010.11.010.

(21) Pérez-Clemente R, Montoliu A, Vives V, López-Climent M, Gómez-Cadenas A. Photosynthetic and antioxidant responses of Mexican lime (Citrus aurantifolia) plants to Citrus tristeza virus infection. Plant Pathol. 2015;64:16-24. Doi: 10.1111/ppa.12241.

(22) Roistacher C. Graft-transmissible diseases of citrus, handbook for detection and diagnosis. Rome: FAO; 1991. 286p.

(23) Bertolini E, Moreno A, Capote N, Olmos A, de Luis A, Vidal E, Pérez-Panadés J, Cambra M. Quantitative detection of Citrus tristeza virus in plant tissues and single aphids by real-time RT-PCR. Eur J Plant Pathol. 2008;120:177-88. Doi: 10.1007/s10658-007-9206-9.

(24) Garnsey S, Gumpf D, Roistacher C, Civerolo E, Lee R, Yokomi R, Bar-Joseph M. Toward standarized evaluation of the biological properties of Citrus tristeza virus. Phytophylactica [Internet]. 1987 [cited 2025 May 2];19:151-7. Available from: https://hdl.handle.net/10520/AJA03701263_997.

(25) van Kooten O, Snel JF. The use of chlorophyll fluorescence nomenclature in plant stress physiology. Photosynth Res. 1990;25(3):147-50. Doi: 10.1007/BF00033156.

(26) Kramer DM, Johnson G, Kiirats O, Edwards GE. New fluorescence parameters for the determination of QA redox state and excitation energy fluxes. Photosynth Res. 2004;79(2):209. Doi: 10.1023/B:PRES.0000015391.99477.0d.

(27) Dhindsa S, Matowe W. Drought tolerance in two mosses: correlated with enzymatic defense against lipid peroxidation. J Exp Bot. 1981;32:79-91. Doi: 10.1093/jxb/32.1.79.

(28) Ramel F, Sulmon C, Bogard M, Couée I, Gouesbet G. Differential patterns of reactive oxygen species and antioxidative mechanisms during atrazine injury and sucrose-induced tolerance in Arabidopsis thaliana plantlets. BMC Plant Biol. 2009;9:28. Doi: 10.1186/1471-2229-9-28.

(29) Sánchez-Rangel JC, Benavides J, Heredia JB, Cisneros-Zevallos L, Jacobo-Velázquez DA. The Folin–Ciocalteu assay revisited improvement of its specificity for total phenolic content determination. Anal Methods. 2013;5:5990-9. Doi: 10.1039/C3AY41125G.

(30) Bradford MM. A rapid and sensitive method for the quantitation of microgram quantities of protein utilizing the principle of protein-dye binding. Anal Biochem. 1976;72:248-54. Doi: 10.1016/0003-2697(76)90527-3.

(31) Rao MV, Paliyath G, Ormrod DP. Ultraviolet-B- and ozone-induced biochemical changes in antioxidant enzymes of Arabidopsis thaliana. Plant Physiol. 1996;110(1):125-36. Doi: 10.1104/pp.110.1.125.

(32) Nakano Y, Asada K. Hydrogen peroxide is scavenged by ascorbate-specific peroxidase in spinach chloroplasts. Plant Cell Physiol. 1981;22:867-80. Doi: 10.1093/oxfordjournals.pcp.a076232.

(33) Rubio L, Arruabarrena A, Salvo M, Castells M, Bertalmío A, Hernández-Rodríguez L, Benítez-Galeano MJ, Maeso D, Colina R, Rivas F. Biological and molecular characterization of a resistance-breaking isolate of citrus tristeza virus from Uruguay and its effects on Poncirus trifoliata growth performance. Arch Virol. 2023;168(4):123. Doi: 10.1007/s00705-023-05749-y.

(34) Harper SJ, Cowell SJ, Robertson CJ, Dawson WO. Differential tropism in roots and shoots infected by Citrus tristeza virus. Virology. 2014;460-461:91-9. Doi: 10.1016/j.virol.2014.04.035.

(35) Tatineni S, Dawson WO. Enhancement or attenuation of disease by deletion of genes from Citrus tristeza virus. J Virol. 2012;86(15):7850-7. Doi: 10.1128/JVI.00916-12.

(36) Tatineni S, Robertson CJ, Garnsey SM, Bar-Joseph M, Gowda S, Dawson WO. Three genes of Citrus tristeza virus are dispensable for infection and movement throughout some varieties of citrus trees. Virology. 2008;376(2):297-307. Doi: 10.1016/j.virol.2007.12.038.

(37) Cook G, van Vuuren SP, Breytenbach JHJ, Steyn C, Burger JT, Maree HJ. Characterization of Citrus tristeza virus single-variant sources in grapefruit in greenhouse and field trials. Plant Dis. 2016;100(11):2251-6. Doi: 10.1094/PDIS-03-16-0391-RE.

(38) Hančević K, Tomislav R, Paskovic I, Urlić B. Biochemical and physiological responses to long-term Citrus tristeza virus infection in Mexican lime plants. Plant Pathol. 2018;67(4):987-94. Doi: 10.1111/ppa.12799.

(39) Björkman O, Demmig B. Photon yield of O2 evolution and chlorophyll fluorescence characteristics at 77 K among vascular plants of diverse origins. Planta. 1987;170(4):489-504. Doi: 10.1007/BF00402983.

(40) Sampol B, Bota J, Riera D, Medrano H, Flexas J. Analysis of the virus-induced inhibition of photosynthesis in malmsey grapevines. New Phytol. 2003;160(2):403-12. Doi: 10.1046/j.1469-8137.2003.00882.x.

(41) Pérez-Clemente RM, Montoliu A, Vives-Peris V, Arbona V, Gómez-Cadenas A. Hormonal and metabolic responses of Mexican lime plants to CTV infection. J Plant Physiol. 2019;238:40-52. Doi: 10.1016/j.jplph.2019.05.001.

(42) Muir CD. A Stomatal model of anatomical tradeoffs between gas exchange and pathogen colonization. Front Plant Sci. 2020;11:518991. Doi: 10.3389/fpls.2020.518991.

(43) Munir N, Hameed AA, Haq R, Naz S. Biochemical changes in cultivars of sweet oranges infected with citrus tristeza virus. Braz J Biol. 2019;79(4):742-8. Doi: 10.1590/1519-6984.193791.

(44) Kaur S, Samota MK, Choudhary M, Choudhary M, Pandey AK, Sharma A, Thakur J. How do plants defend themselves against pathogens-Biochemical mechanisms and genetic interventions. Physiol Mol Biol Plants. 2022;28(2):485-504. Doi: 10.1007/s12298-022-01146-y.

(45) Siddique Z, Akhtar KP, Hameed A, Sarwar N, Imran-Ul-Haq, Khan SA. Biochemical alterations in leaves of resistant and susceptible cotton genotypes infected systemically by cotton leaf curl Burewala virus. J Plant Interact. 2014;9:702-11. Doi: 10.1080/17429145.2014.905800.

(46) Zhao S, Li Y. Current understanding of the interplays between host hormones and plant viral infections. PLoS Pathog. 2021;17(2):e1009242. Doi: 10.1371/journal.ppat.1009242.

(47) Padmanabhan MS, Goregaoker SP, Golem S, Shiferaw H, Culver JN. Interaction of the tobacco mosaic virus replicase protein with the Aux/IAA protein PAP1/IAA26 is associated with disease development. J Virol. 2005;79(4):2549-58. Doi: 10.1128/JVI.79.4.2549-2558.2005.